Supplementary Data:

Microglia and macrophages promote corralling, wound compaction and recovery after spinal cord injury via Plexin-B2

Xiang Zhou [1,4,*], Shalaka Wahane [1,*], Marie-Sophie Friedl [6], Michael Kluge [6], Caroline C. Friedel [6], Kleopatra Avrampou [1], Venetia Zachariou [1,3], Xijing He [4,5], Roland H. Friedel [1,2,#], and Hongyan Zou [1,2,#]

[1] Nash Family Department of Neuroscience, [2] Department of Neurosurgery, Friedman Brain Institute, [3] Department of Pharmacological Sciences, Icahn School of Medicine at Mount Sinai, New York, New York, USA, [4] Department of Orthopedics, Second Affiliated Hospital of Xi'an Jiaotong University, [5] Xi'an International Medical Center, Xi'an, Shaanxi, China, [6] Institut für Informatik, Ludwig-Maximilians-Universität München, Munich, Germany

Supplementary Figures 1-8

Supplementary Video Legends 1-8

Supp. Fig. 1

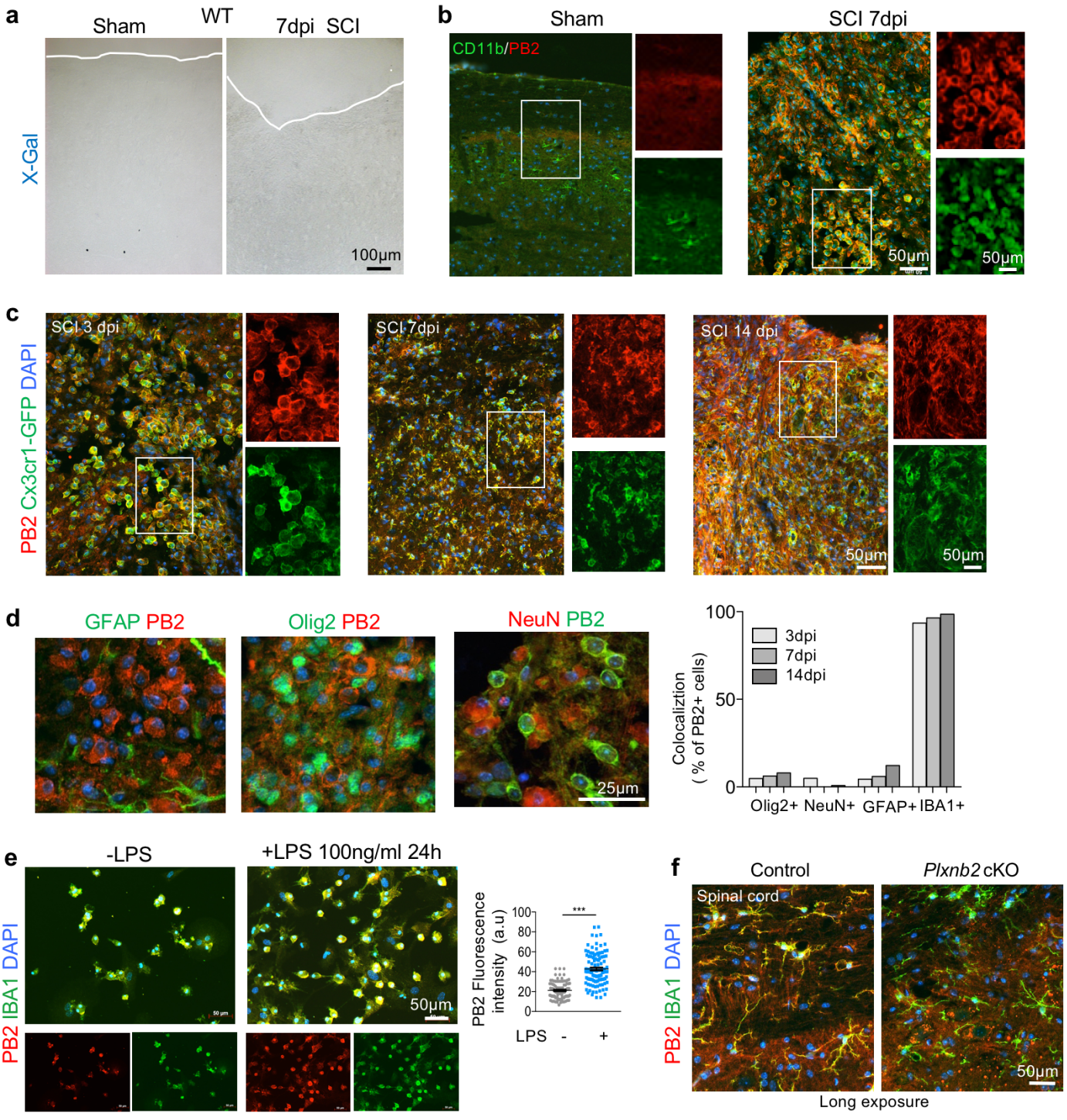
a
Sham
WT
7dpi SCI
X-Gal
100μm
b
Sham
SCI 7dpi
CD11b/PB2
50μm
50μm
c
SCI 3 dpi
SCI 7dpi
SCI 14 dpi
PB2 Cx3cr1-GFP DAPI
50μm
50μm
d
GFAP PB2
Olig2 PB2
NeuN PB2
25μm
Colocaliztion (% of PB2+ cells)
3dpi
7dpi
14dpi
Olig2+ NeuN+ GFAP+ IBA1+
e
-LPS
+LPS 100ng/ml 24h
PB2 IBA1 DAPI
50μm
PB2 Fluorescence intensity (a.u)
LPS - +
f
Control
Plxnb2 cKO
Spinal cord
PB2 IBA1 DAPI
50μm
Long exposure

Supplementary Figure 1. Upregulation of Plexin-B2 in activated microglia/macrophages after SCI.

a. X-Gal staining of sagittal section of thoracic spinal cords from WT mouse show negative lacZ activity in sham or after SCI at 7 dpi. Images from 3 independent mice for each condition showed similar results. **b.** IHC images show Plexin-B2 induction at the injury site at 7 dpi after SCI, which co-localizes with CD11b. Images from 4 independent mice for each condition showed similar results. **c.** IHC images of thoracic spinal cords from *Cx3cr1*^{GFP} reporter mice show co-localization of Plexin-B2 and GFP at three time points after T8 transection. Images from 4 independent mice for each condition showed similar results. **d.** IHC images show minimal overlap between Plexin-B2 and the indicated neural markers at the injury site after SCI. Quantifications demonstrate that Plexin-B2 upregulation largely occurs in IBA1^{+} microglia/macrophages at three time points after SCI. Images from 4 independent mice showed similar results. **e.** Immunostaining of primary microglia (IBA1^{+}) isolated from *Cx3cr1*^{CreER} *Plxnb2*$^{fl/B}$ mice with no Tamoxifen exposure show Plexin-B2 induction upon LPS stimulation. Quantifications are shown on the right. n=100 cells counted from 3 independent cultures for each condition, unpaired two-tailed Student's t test, ***p<0.0001. Data represent mean ± SEM. **f.** IHC images with long exposure show baseline expression of PB2 that colocalizes with IBA1 in uninjured spinal cord in control mice, but ablation of Plexin-B2 in *Plxnb2* cKO mice. Images from 4 independent mice for each condition showed similar results.

Supp. Fig. 2

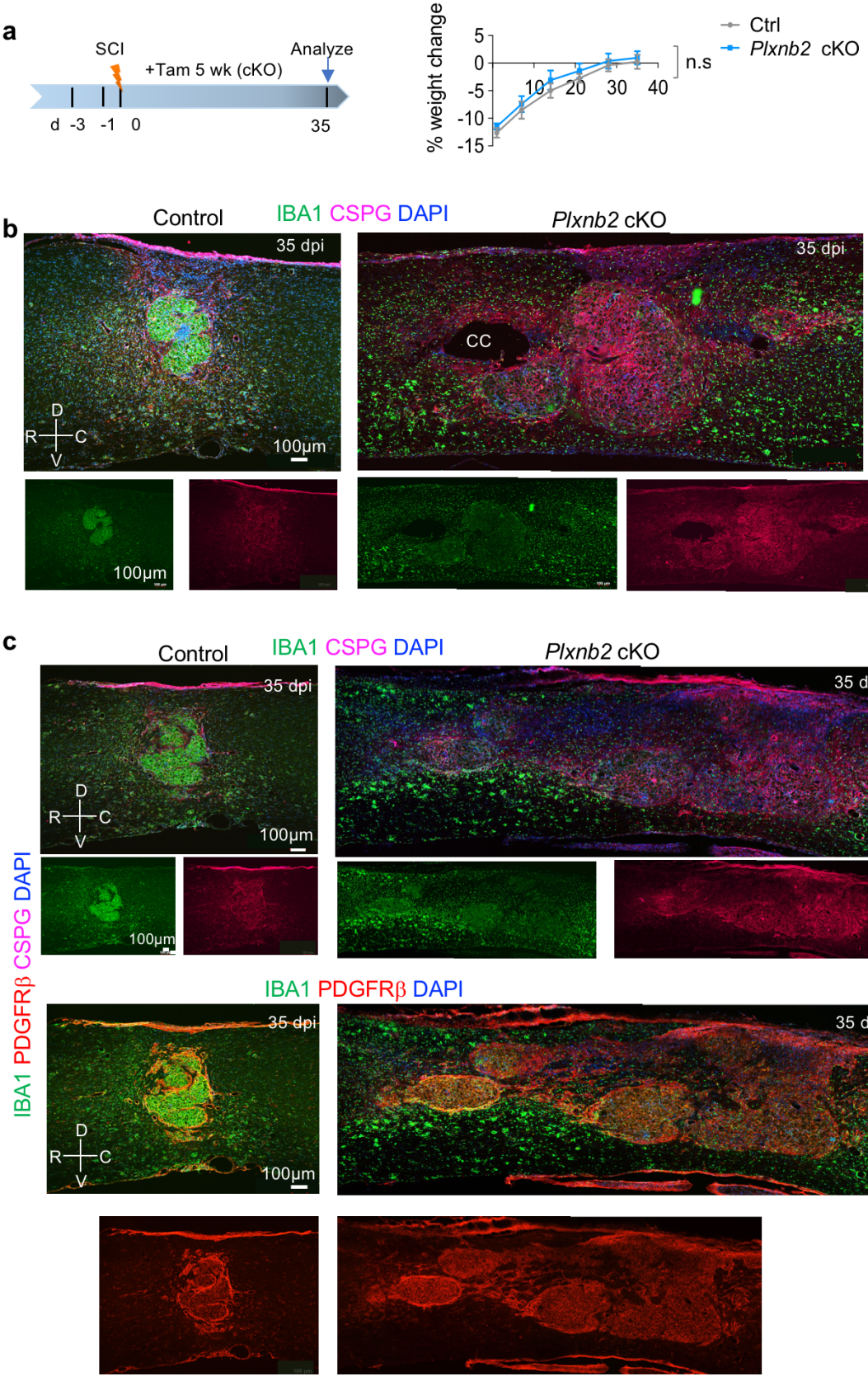
a
SCI
Analyze
+Tam 5 wk (cKO)
d -3 -1 0
35
% weight change
5
0
-5
-10
-15
10 20 30 40
n.s
Ctrl
Plxnb2 cKO
b
Control
IBA1 CSPG DAPI
Plxnb2 cKO
35 dpi
CC
D
R
C
V
100μm
c
IBA1 CSPG DAPI
IBA1 PDGFRβ DAPI

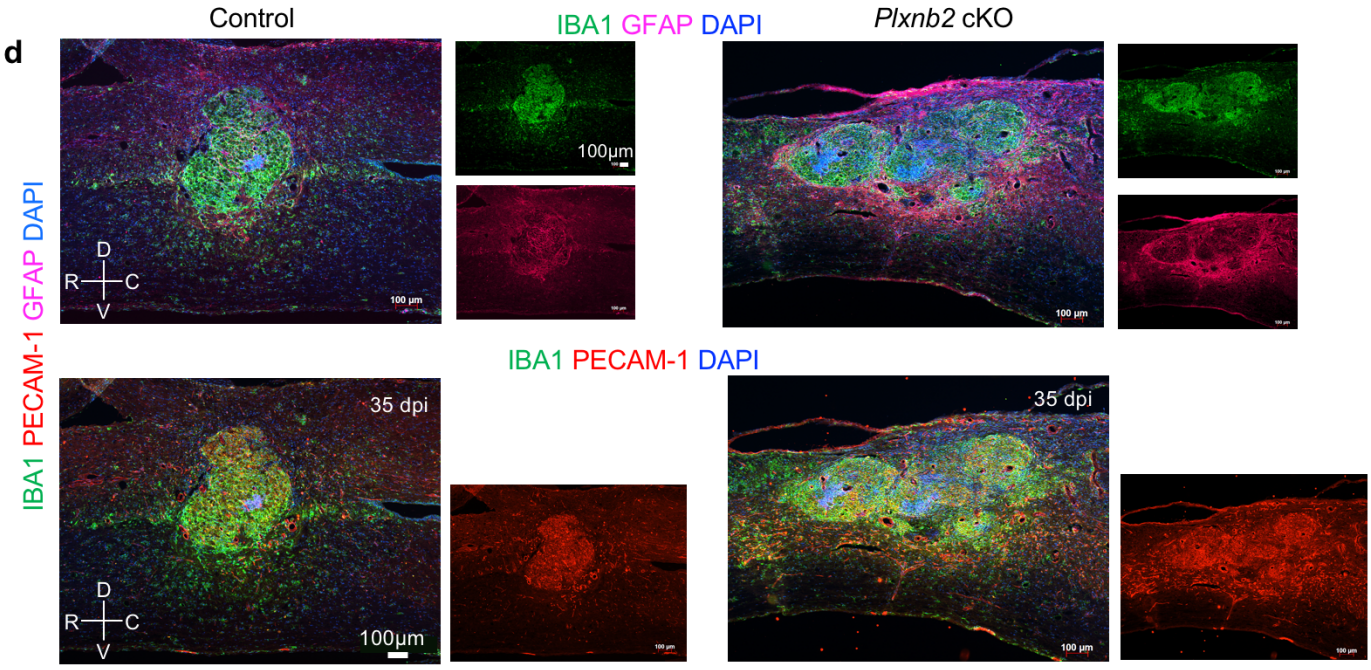

Supplementary Figure 2. Plexin-B2 ablation in IAM impairs wound healing.

a. Left, experimental scheme with continuous tamoxifen injection from 3 days before until 5 weeks after SCI. Right, graphs show no signification difference in body weight between cohorts during recovery after SCI. n=8 animals per group, two-way ANOVA with Bonferroni post hoc correction, n.s., p=0.11. Data represent mean ± SEM. **b.** IHC of sagittal thoracic spinal cords show much expanded distribution of IBA1$^+$ cells and CSPGs, detected by CS-56 antibody, in *Plxnb2* cKO as compared to control mice. Note the same spinal cord tissue was used for these co-staining as in Fig. 4b. **c.** IHC of sagittal thoracic spinal cords show expanded territory of pericytes (PDGFRβ$^+$) together with IBA1$^+$ immune cells as well as CSPG deposits in spatial disarray at the lesion site in *Plxnb2* cKO as compared to control mice at 35 dpi. **d.** IHC of sagittal thoracic spinal cords show engorged blood vessels in expanded territory in cKO at 35 dpi, in contrast to the largely regressed capillary at the injury penumbra in control animal. R-rostral; C-caudal; D-dorsal; V-ventral, CC-central canal. For **b, c,** and **d**, n=3 independent mice per genotype with similar results.

Supp. Fig. 3

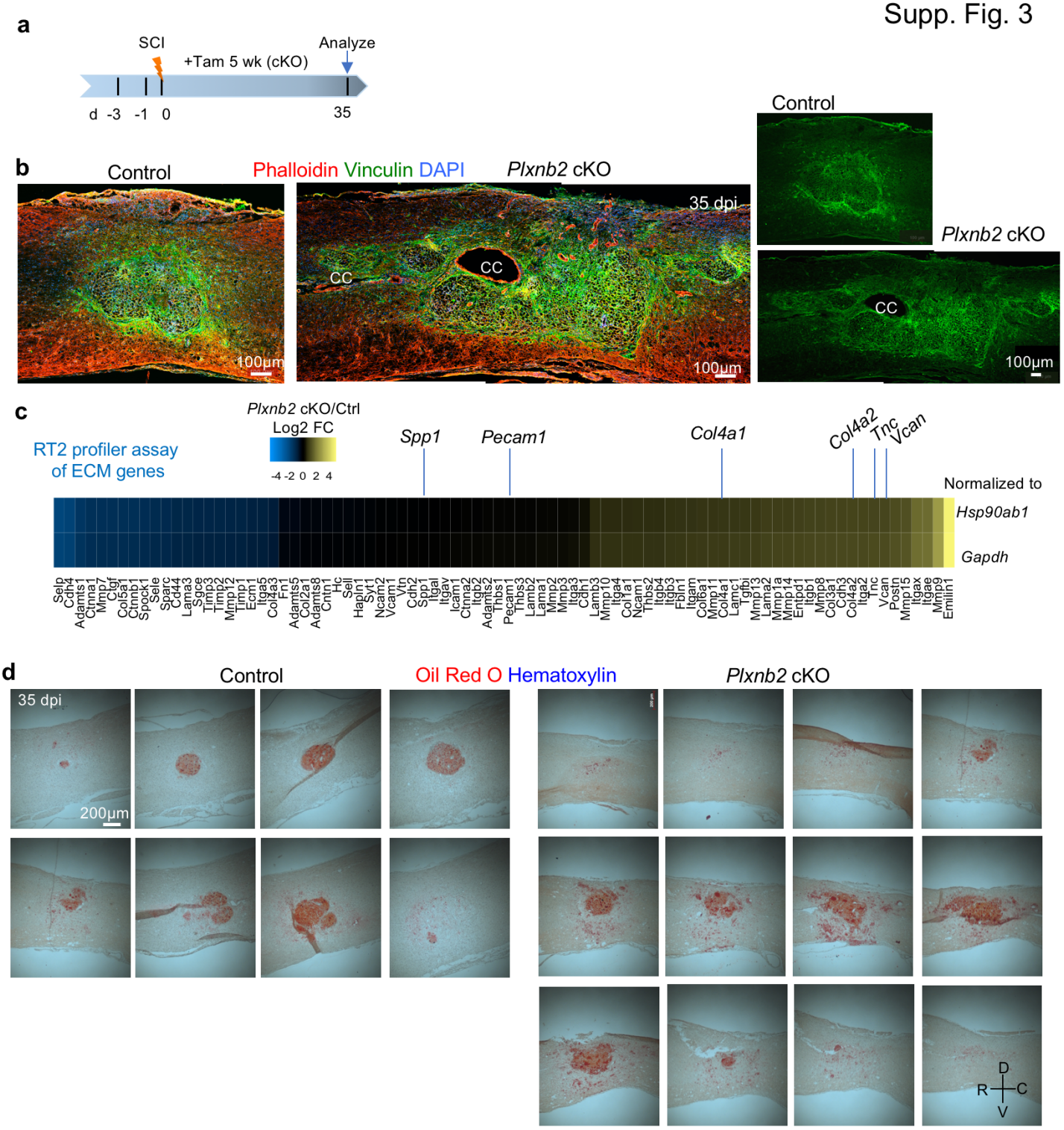

Supplementary Figure 3. Plexin-B2 ablation in IAM impairs wound healing.
a. Experimental scheme with continuous tamoxifen exposure from 3 days before until 5 weeks after SCI. **b.** IHC of sagittal thoracic spinal cords show high level of Vinculin at the lesion core, which is widespread in *Plxnb2* cKO mice. Phalloidin staining also show engorged blood vessels in cKO but capillary regression in control. Images were obtained from two independent pairs of mice with similar results. **c.** Transcriptional profiling of ECM genes at the injury site in *Plxnb2* 2 cKO mice relative to control littermates at 14 dpi. Heatmap denotes log2 fold change (FC). Data from using two house keeping genes, *Gapdh* or *Hsp90ab1*, show similar results. The ECM genes validated in IHC are highlighted. **d.** Images of consecutive sagittal sections of thoracic spinal cords show widespread Oil Red O staining in *Plxnb2* cKO mice at 35 dpi as compared to the confined lipid debris at the lesion core in littermate controls. Images obtained from three independent mice per group showed similar results. R-rostral; C-caudal; D-dorsal; V-ventral, CC-central canal.

Supp. Fig. 4

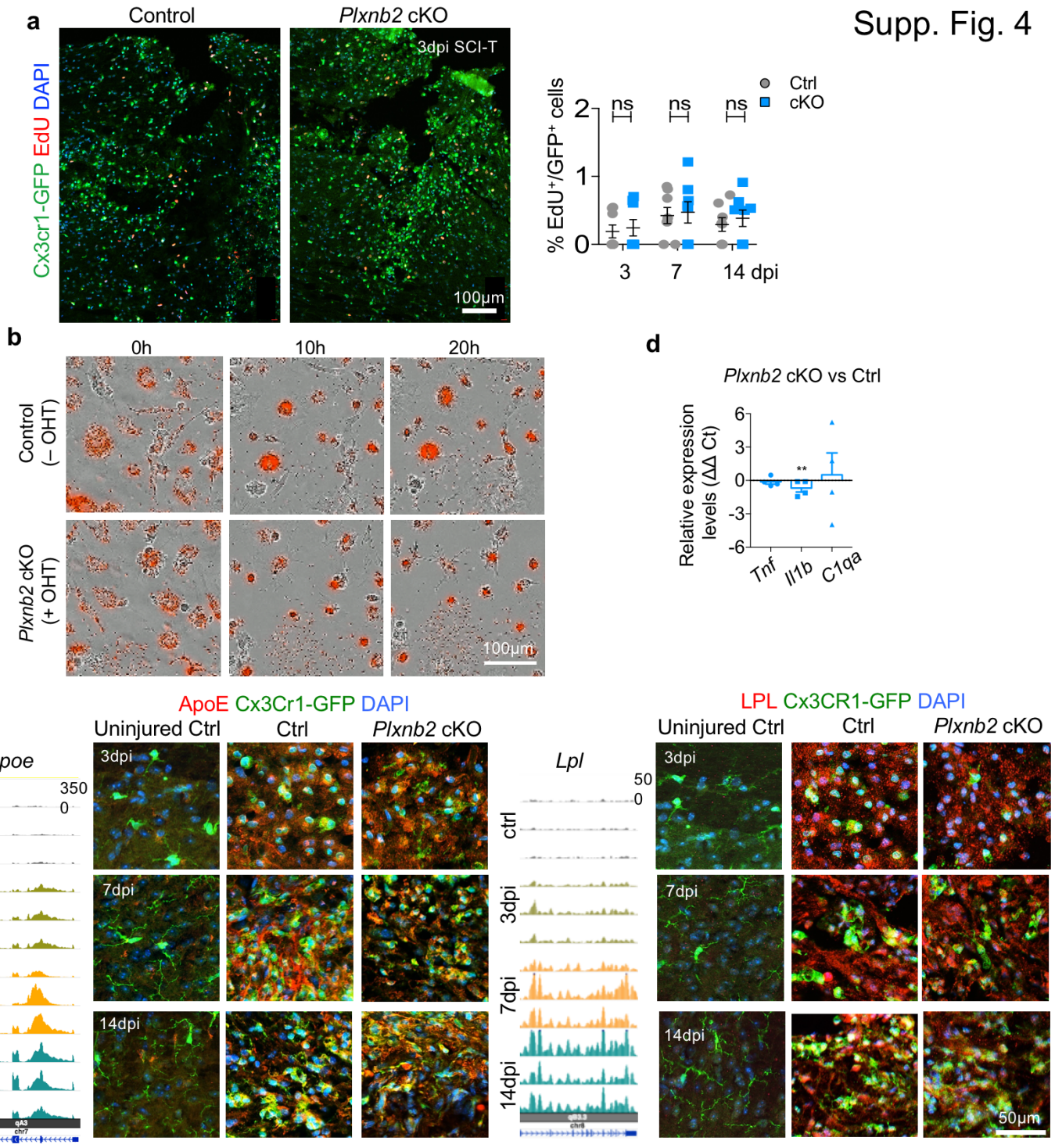

Supplementary Figure 4. Plexin-B2 ablation does not affect immune-related core function of IAM.
a. IHC images of thoracic spinal cords at 3 dpi after T8 dorsal transection (SCI-T). Mice also carry the *Cx3cr1*^{GFP} reporter. EdU was delivered 3 hours before tissue harvest. Quantifications are shown on the right. Unpaired two-tailed Student's t test. For 3 dpi, n=4 animals, n.s., p=0.62. For 7 dpi, n=4 animals, p=0.81. For 14 dpi, n=5 animals, p= 0.57. Data represent mean ± SEM. **b.** Images of phagocytosis assays show that both control (no hydroxy-tamoxifen) and *Plxnb2* cKO (with hydroxy-tamoxifen) microglia are capable of phagocytosing fluorescent beads. n=3 independent cultures with similar results. **c.** Read coverage tracks from RNA-Seq data and IHC images illustrate similar upregulation of the two lipid metabolism genes in IAM in control and *Plxnb2* cKO mice at three time points after SCI. Images from 3 independent mice per condition revealed similar results. **d.** qRT-PCR results show relative expression levels of the indicted cytokines in log2 fold change in mixed cortical cultures of the indicated genotypes. *Gapdh* was used as house keeping gene. n=4 independent culture samples, each performed in triplicates, unpaired two-tailed Student's t test, p=0.43 for *Tnf,* **p=0.0050 for *Il1b,* and p=0.86 for *C1qa.*

Supp. Fig. 5

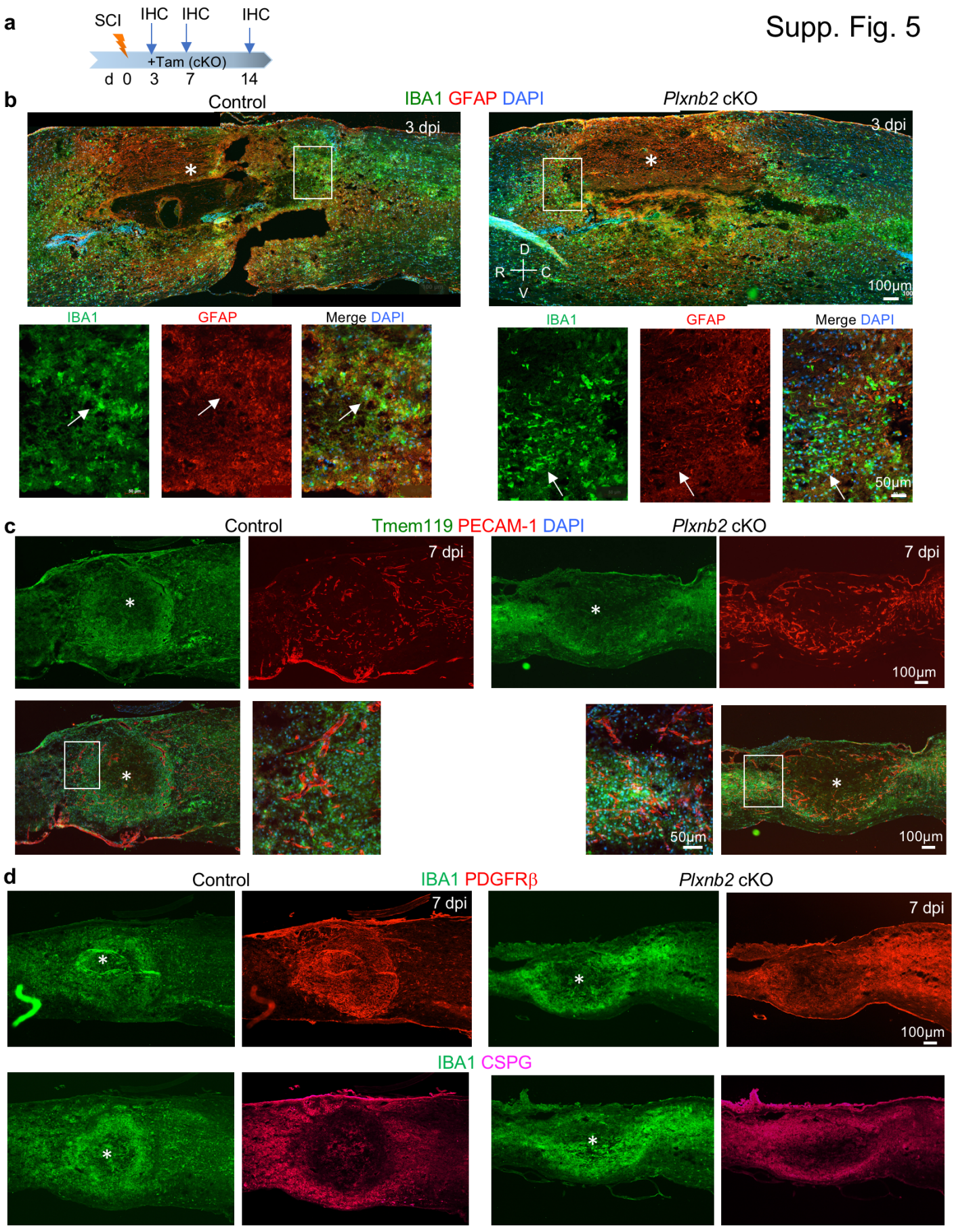
a
SCI
IHC
IHC
IHC
+Tam (cKO)
d 0 3 7 14
b
Control
IBA1 GFAP DAPI
Plxnb2 cKO
3 dpi
3 dpi
D
R
C
V
100μm
IBA1
GFAP
Merge DAPI
IBA1
GFAP
Merge DAPI
50μm
c
Control
Tmem119 PECAM-1 DAPI
Plxnb2 cKO
7 dpi
7 dpi
100μm
50μm
100μm
d
Control
IBA1 PDGFRβ
Plxnb2 cKO
7 dpi
7 dpi
100μm
IBA1 CSPG

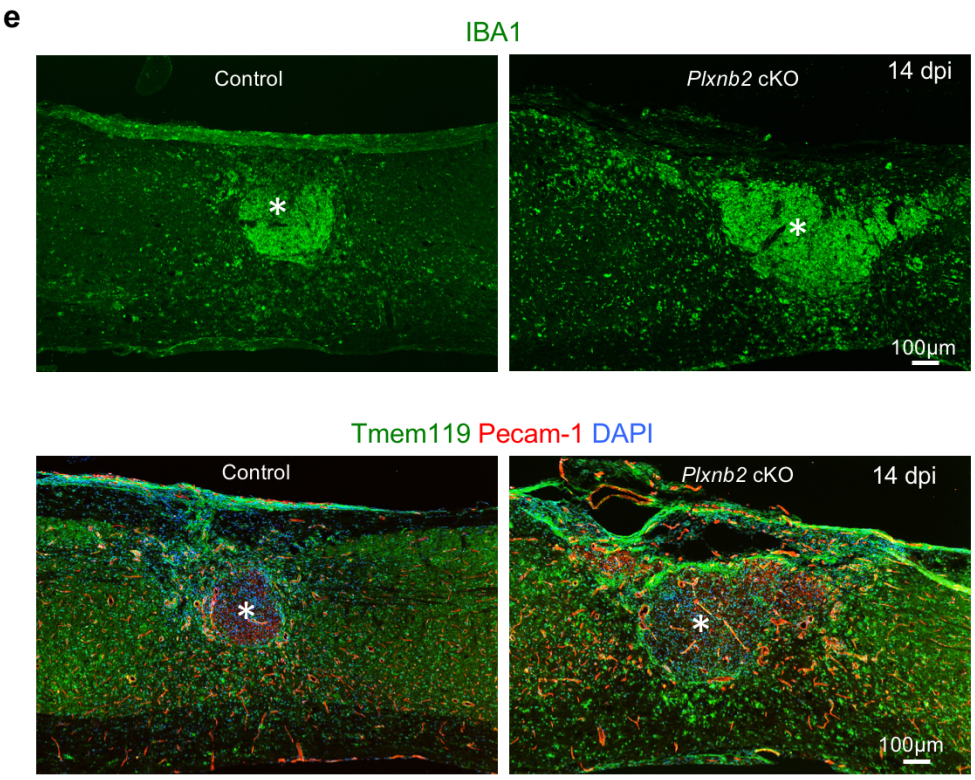

Supplementary Figure 5. Plexin-B2 in IAM is required for corralling and vascular organization after SCI.
a. Experimental scheme. Tamoxifen was injected from day 3 before SCI until the time of analysis. (**b-e**) IHC images of sagittal thoracic spinal cords show early onset of the corralling process after T8 contusion injury. **b.** Note that in control mice at 3 dpi, dispersion of IBA1$^+$ immune cells and intermingling with GFAP$^+$ cells at the injury site, however, in *Plxnb2* cKO mice, IBA1$^+$ cells tended to cluster together (white arrows). **c.** Note the different orientation of the neovasculatures at the lesion site in *Plxnb2* cKO mice, as compared to the concentric neovascular pattern in control at 7 dpi. Enlarged images of boxed area are shown on right. **d.** In control animal, by 7 dpi, pericytes (PDGFRβ^+) had formed a ringed pattern at the injury site, in close alignment with IBA1+ cells and surrounded by CSPGs at the lesion penumbra, whereas in *Plxnb2* cKO animal, pericytes had expanded their territories that mirrored the spatial disarray of IBA1+ cells, so were CSPGs. **e.** Note regression of capillary at the injury site in control, but persistent engorged blood vessels in cKO animal at 14 dpi. White asterisks denote the lesion core. R-rostral; C-caudal; D-dorsal; V-ventral. Images from 2 (for **d**) or 3 (for **b, c,** and **e)** independent mice per genotype showed similar results.

Supp. Fig. 6

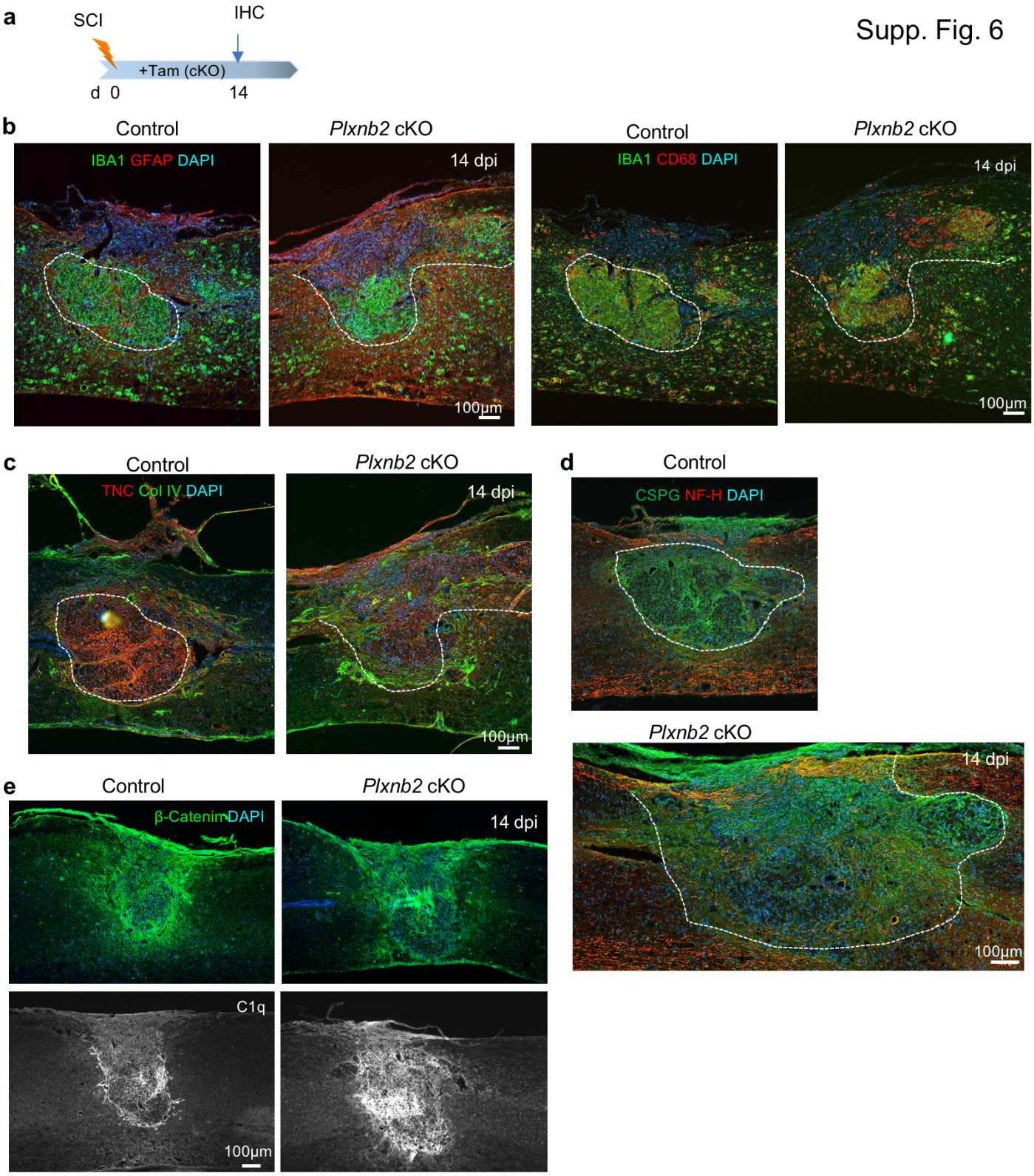

Supplementary Figure 6. Plexin-B2 in IAM is required for corralling and matrix reorganization after SCI.

a. Experimental scheme. Tamoxifen was injected from day 3 before until 2 weeks after SCI. (**b-e**) Representative IHC images of sagittal thoracic spinal cords at 14 dpi stained for the indicated genes show impair corralling and matrix disorganization in *Plxnb2* cKO mice after T8 contusion injury. Lesion site appeared enlarged and C1q widespread in cKO mice. White dashed lines denote lesion border. R-rostral; C-caudal; D-dorsal; V-ventral. For **b, c, d** and **e,** images obtained from 3 independent mice per genotype showed similar results.

Supp. Fig. 7

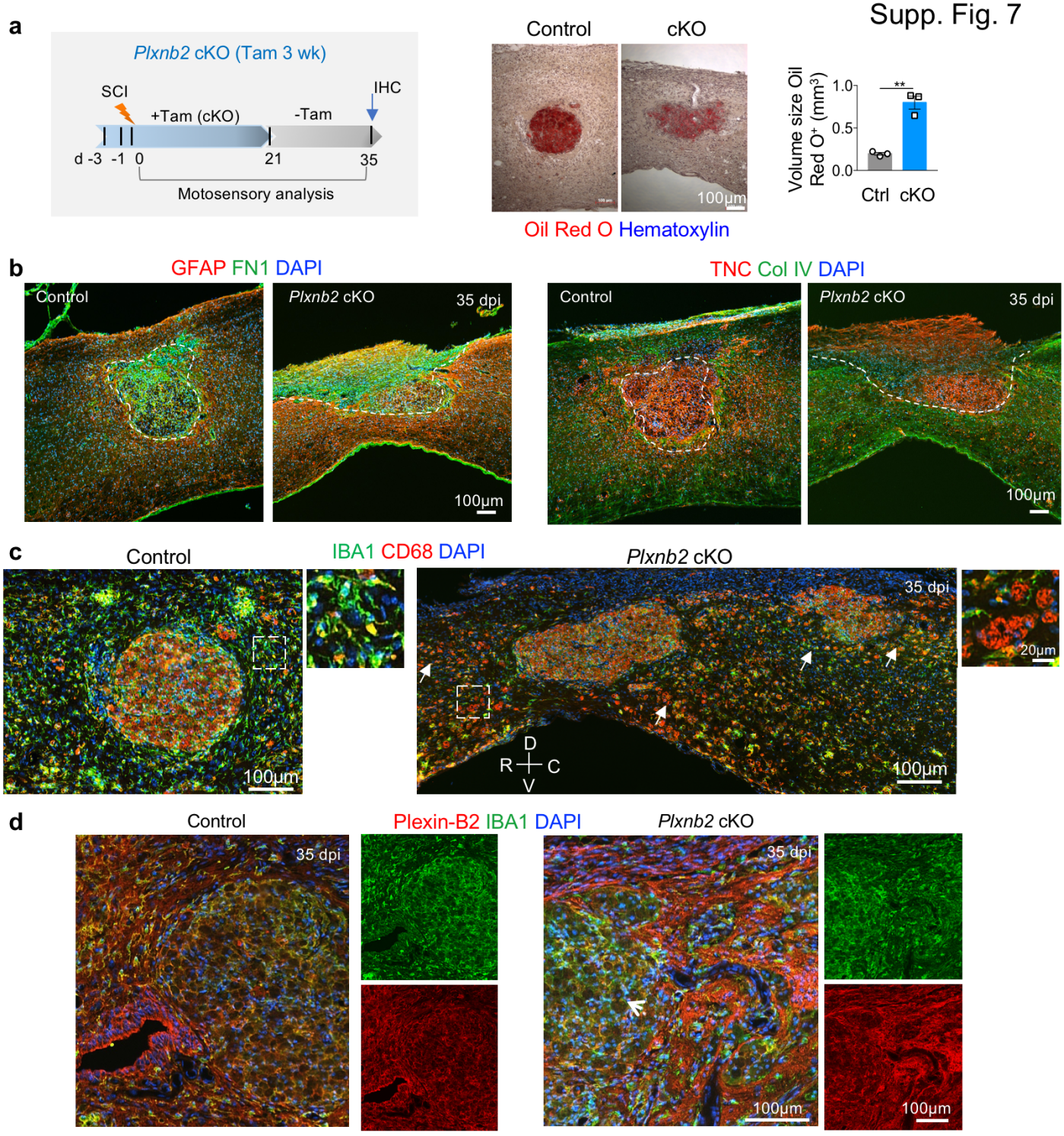

Supplementary Figure 7. Plexin-B2 in IAM is critical for corralling and injury resolution during the early phase of recovery from SCI.

a. Left, experimental scheme. Tamoxifen was injected from day 3 before until 3 weeks after SCI. Middle, Images of sagittal section of thoracic spinal cords show confined Oil Red O staining in control but diffuse in Plexin-B2 cKO mice at 35 dpi. Quantifications are shown on the right, n=3 animals per group, unpaired two-tailed Students t-test, **p=0.0015. Graphs represent mean ± SEM. **b-d.** IHC of sagittal thoracic spinal cords at 35 dpi stained for the indicated markers show impaired corralling and matrix disorganization in *Plxnb2* cKO mice. **b.** White dashed lines denote lesion border. **c.** Note widespread CD68^{+} cells (white arrows) in *Plxnb2* cKO mice at 35 dpi. Enlarged images of boxed areas are shown on the right. **d.** Note with this tamoxifen regimen, in *Plxnb2* cKO mice at 35 dpi, re-expression of Plexin-B2 in newly infiltrated macrophages at the injury site, while microglia continue to have Plexin-B2 ablation (white arrowhead). R-rostral; C-caudal; D-dorsal; V-ventral. For **b, c,** and **d**, n=3 independent mice per genotype with similar results.

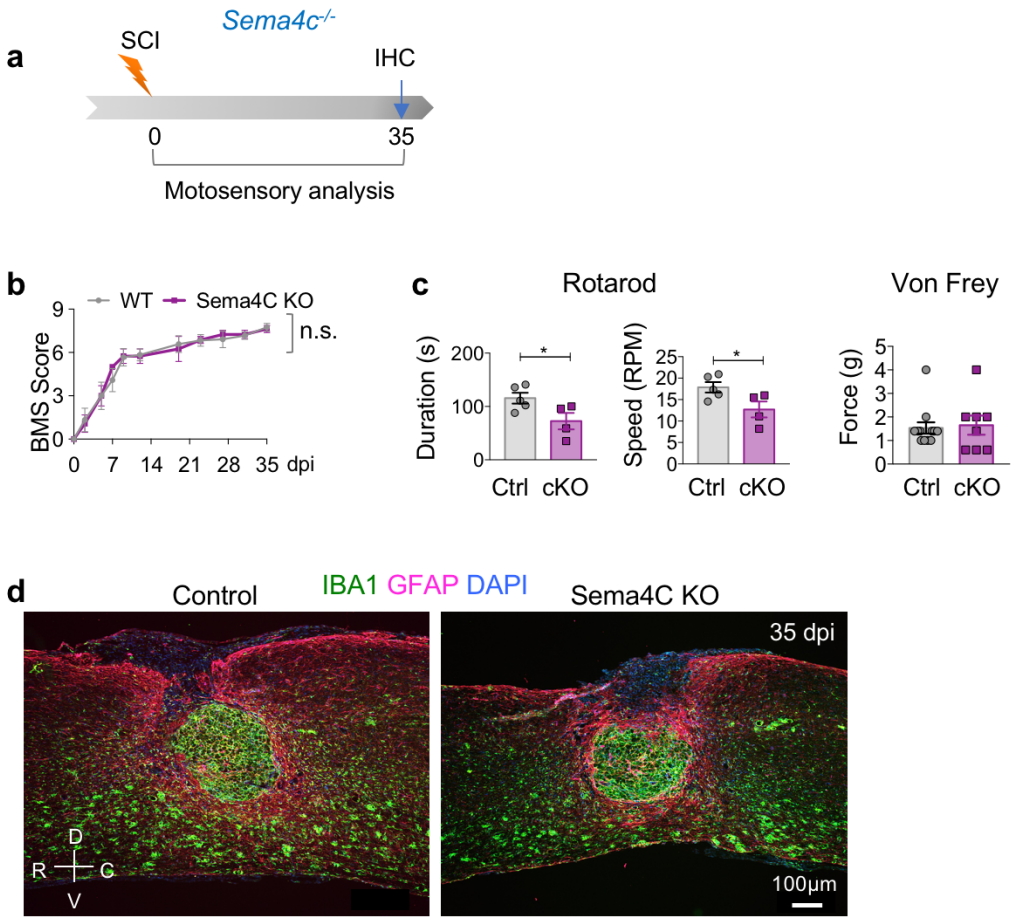

Supplementary Figure 8. Sema4C knockout minimally impacts functional recovery and wound healing after SCI.

a. Top, experimental scheme. **b.** BMS scores during the 5 week recovery after T8 contusion injury demonstrate comparably functional recovery in Sema4C KO mice as compared to littermate controls. n=6 for control cohort, n=4 for cKO cohort. Two-way ANOVA with Bonferroni post hoc correction for repeated measures. n.s., p=0.72. Data represent mean ± SEM. **c.** Rotarod test showed a modest decrease of hindlimb and tail balance in Sema4C KO mice as compared to littermate controls (n=5 for control cohort, n=4 for cKO cohort). Unpaired two-tailed Student's t test. For duration, *p=0.046; for speed, *p=0.046. Von Frey filament test showed no significant difference in tactile sensory function between genotypes (n=5 for control cohort, n=4 for cKO cohort). For each animal, left and right hindpaws measured separately. Unpaired two-tailed Student's t test. p=0.79. Data represent mean ± SEM. **d.** IHC images of sagittal thoracic spinal cord at 35 dpi stained for the indicated markers show successfully corralling and wound compaction in both cohorts after T8 contusion injury. Images from 3 animals per genotype showed similar results. R-rostral; C-caudal; D-dorsal; V-ventral.

Supplemental Video Legends

Supplementary Video 1. Open field BMS scoring for control animal.

Open field walking test for BMS scoring of a control animal at 35 days post injury. Animals were scored for plantar placement, ankle movement, angle of hindlimbs, trunk stability and other parameters as outlined in the BMS guidelines previously published. One representative movie from 12 independent animals shown.

Supplementary Video 2. Open field BMS scoring for *Plxnb2* cKO animal.

Open field walking test for BMS scoring of a *Plxnb2* cKO animal at 35 days post injury. One representative movie from 12 independent animals shown.

Supplementary Video 3 and 4. Phagocytosis assay.

pHrodo red zymosan bioparticles were added to a lawn of microglia isolated from *Plxnb2*$^{fl/B}$ *Cx3cr1*$^{CreER/GFP}$ mice without (control) or with tamoxifen treatment (cKO). In both conditions, cells phagocytosed the beads comparably. IncuCyte time-lapse movies were acquired at 1 hour intervals for a period of 24 hours. n=3 independent cultures per condition showed similar results.

Supplementary Video 5. Cell motility for control microglia.

Control microglia (GFP^{+}) are highly motile. Primary microglia from cortex of neonatal *Plxnb2*$^{fl/B}$ *Cx3cr1*$^{CreER/GFP}$ pups were harvested and cultured. Cx3cr1-GFP^{+} microglia were overlaid on a lawn of Cx3cr1-GFP^{-} neural cells (labeled with CellTracker Red). IncuCyte time-lapse movie was acquired at 30 min intervals, for a duration of 5 days. Microglia motility (red line) was tracked using the MTrackJ plugin from ImageJ. n=3 independent cultures showed similar results.

Supplementary Video 6. Cell motility for *Plxnb2* cKO microglia.

Plxnb2 cKO microglia (GFP^{+}) tracked on a lawn of neural cells labeled with CellTracker Red, as in Supplementary Video. n=3 independent cultures showed similar results.

Supplementary Video 7. Contact inhibition of locomotion (CIL) of control microglia.

IncuCyte time-lapse movie was acquired at 5 minute time intervals over a period of 2 hours. Only 30 min clip is shown here. Cortical cultures were obtained from neonatal *Plxnb2*$^{fl/B}$ *Cx3cr1*$^{CreER/GFP}$ mice and were not treated with OHT (control). Microglia were visualized by Cx3cr1-GFP reporter labels. Control microglia retracted and moved away within 5 minutes of contact with other cell types. n=3 independent cultures showed similar results.

Supplementary Video 8. Contact inhibition of locomotion (CIL) of *Plxnb2* cKO microglia.

IncuCyte time-lapse movie was acquired at 5 minute time intervals over a period of 2 hours. Only 30 min clip is shown here. Cortical cultures were obtained from neonatal *Plxnb2*$^{fl/B}$ *Cx3cr1*$^{CreER/GFP}$ mice and treated with OHT (*Plxnb2* cKO). Microglia were visualized by Cx3cr1-GFP reporter label. Mutant cKO microglia stayed longer in contact with other cells than in control conditions. n=3 independent cultures showed similar results.